Hot-Film Anemometry Measurements of Turbulence in Pipe Flow: Organic Solvents

GARY K. PATTERSON and JACQUES L. ZAKIN

University of Missouri at Rolla, Rolla, Missouri

Longitudinal turbulence intensities, autocorrelations, and energy spectra have been measured in the flow of toluene, benzene, and cyclohexane in smooth, round 1- and 2-in. I.D. tubes. These measurements were made with a constant-temperature hot-film anemometer and covered radial positions from the center to $r/a = 0.85$ in the 2-in. tube and to $r/a = 0.75$ in the 1-in. tube.

The turbulence intensity data were found to be similar to those obtained for air in a 10-in. pipe by Laufer. A slight diameter effect was observed, the intensities in the 1-in. tube being slightly lower than those in the 2-in. tube at equal Reynolds numbers.

The energy spectra were similar to the spectrum reported by Lee and Brodkey for water. The spectra reached higher frequencies at the lowest measurable energy levels for higher velocities. There was little effect of tube diameter or radial position on the spectra from the center to $r/a = 0.85$. A short inertial subrange with a log-log slope of $-5/3$ seemed evident in high velocity spectra, and the log-log slope of -7 was approached at high frequencies by the lowest velocity spectrum.

The peak energy dissipation frequencies for all the energy spectra measured were approximately proportional to bulk mean velocity to the 1.4 power with little effect of tube diameter or radial position from the center to $r/a = 0.85$.

Integral scales of the turbulence were proportional to bulk mean velocity to a power less than one for a given tube. These measurements indicated that the ratio of integral scale to pipe diameter is not a function of Reynolds number only.

Microscale values were relatively independent of velocity and pipe diameter.

The great interest in drag reduction in turbulent flow in pipes [see review by Hershey (*1*)] has led to an interest in liquid pipe flow turbulence in general (*2*). Increased knowledge of the fluctuations of velocity and pressure in liquid turbulence in pipes will provide a basis for interpreting drag reduction measurements and also contribute to the general knowledge of pipe flow. Most measurements of fluctuating velocity and pressure in pipes have been made in air where hot-wire anemometers could be used.

The aim of this paper is to discuss the theoretical basis for turbulence measurements in liquids, present data for such measurements in organic solvents, and compare them with other data available.

By Reynolds averaging (*3*) the Navier-Stokes equations the following equations are obtained for pipe flow:

$$\overline{u'v'} = \nu \frac{d\bar{u}}{dr} + \frac{r}{a}(u^*)^2 \tag{1}$$

$$-\overline{(v')^2} + \int_o^r \frac{\overline{(v')^2} - \overline{(w')^2}}{r}\,dr = \frac{(\bar{p} - p_0)}{\rho} + \frac{2(u^*)^2(x - x_0)}{a} \tag{2}$$

where the prime indicates fluctuation and the bar indicates average. When the Reynolds stress $\overline{u'v'}$ is zero, the first equation is simply Newton's law of viscosity for a tube. When the mean-square quantities $\overline{(v')^2}$ and $\overline{(w')^2}$ are zero, the second equation reduces to the expression for wall shear stress $\tau_w = (a\Delta\bar{p}/2\Delta x)$. Although $\overline{(u')^2}$ does not appear in the above equations, it is important in its contribution to the Reynolds stress $\overline{u'v'}$ and is the most commonly measured quantity.

Using air in a 4-in. pipe, Sandborn (*4*) measured all three mean-square fluctuating velocities (turbulence intensities) and the Reynolds stress in a Reynolds number range of 32,000 to 270,000. Using his data, which was obtained with a constant-temperature hot-wire anemometer, he obtained satisfactory confirmation of Equations (1) and (2) for a pipe.

Laufer (*5*) studied the turbulent flow of air in a 10-in. pipe. He used a constant-current hot-wire anemometer for his measurements and found that the peak of both production and dissipation of turbulent energy and also the peak turbulence intensities occurred at $y^+ = 12$.

Additional information about the structure of turbulence may be obtained from the autocorrelation function, which was defined by Taylor (*6*) as follows:

$$R(\tau) = \frac{\overline{u'(t)\,u'(t+\tau)}}{<u'>^2} \tag{3}$$

where $<\ >$ denotes a root-mean-square term. Taylor (*7*) postulated that for $<u'> << \bar{u}$, the autocorrelation function is related to the space correlation function, $f(\delta) = \overline{u'(x)\,u'(x+\delta)}/<u'>^2$, as follows:

$$f(\delta) = R(\delta/\bar{u}) \tag{4}$$

This has been validated experimentally for isotropic turbulence in air by Favre et al. (*8*). Using their boundary-layer data, Sternberg (*9*) showed, however, that the presence of a velocity gradient causes all the large scale vortices to be convected downstream at a velocity slightly lower than the free-stream velocity. Sternberg estimated the convection velocity of the larger vortices to be 0.8 $\bar{u}_x$. If $\bar{u}_x$ is assumed to correspond to $\bar{u}_c$ in a pipe, the large vortex convection velocity in the pipe is then 0.8 $\bar{u}_c$, which is approximately equal to the bulk mean velocity.

The integral scale of turbulence is defined as (3)

$$L_x = \int_o^\infty f(\delta)\,d\delta \tag{5}$$

The integral scale can be expressed in terms of the autocorrelation function for isotropic turbulence:

$$L_x = \int_o^\infty R(\delta/\bar{u})\,d(\tau\bar{u} = \bar{u}\int_o^\infty R(\tau)\,d\tau \tag{6}$$

Since the largest vortices are probably convected more slowly than the centerline velocity in a pipe, and since the integral scale is sensitive primarily to the largest vortices, 0.8 $\bar{u}_c$ should probably replace $\bar{u}$. In practice the upper limit for the integral is generally taken as the point at which $R(\tau)$ first becomes zero.

The longitudinal microscale may be defined as (3)

$$\lambda_f = \delta \xrightarrow{\lim} 0 \frac{\delta}{\sqrt{1 - f(\delta)}} \tag{7}$$

Application of l'Hospital's rule twice to Equation (7) squared gives

$$\lambda_f = \sqrt{-2/[\partial^2 f(\delta)/\partial\delta^2]_{\delta=0}} \tag{8}$$

The one-dimensional energy spectrum of turbulence is defined as $E_x(n) = d\,\langle u'\rangle^2/dn$ or as $F_x(n) = (1/\langle u'\rangle^2)E_x(n)$ when normalized with respect to $\langle u'\rangle^2$ (3). This spectrum has been shown by Taylor (7) to be a Fourier transform of the autocorrelation function times four. Therefore the isotropic turbulent energy dissipation and the longitudinal microscale may be expressed in terms of the energy spectrum (3):

$$W = \frac{60\pi^2\,\nu\,\langle u'\rangle^2}{\bar{u}^2}\int_o^\infty F_x(n)\,n^2\,dn \tag{9}$$

$$\lambda_f = \frac{\bar{u}}{\sqrt{2}\,\pi\sqrt{\int_o^\infty F_x(n)\,n^2\,dn}} \tag{10}$$

According to Kolmogoroff's first similarity hypothesis, high-frequency eddies are less affected by shear than the large-scale motions and therefore approach isotropy (10). Since most of the dissipation occurs at high frequencies, the isotropic energy dissipation should be a good estimate of the dissipation in pipe flow except very near the wall. The use of autocorrelations and the Taylor hypothesis to obtain microscale values for pipe flow [Equation (10)] is justified by the contention of Sternberg that the smaller vortices move with the local time mean velocity.

Kolmogoroff's second similarity hypothesis leads to the inertial subrange with a −5/3 log-log slope, the same as Heisenberg's (11) transfer theory, which also predicts a limiting high wave number log-log slope of −7. Both these similarity hypotheses have been supported by the measurements of Gibson and Schwarz (12) in isotropic grid turbulence. They found that an inertial subrange with a log-log slope of −5/3 occurred at turbulence microscale Reynolds numbers ($N_{Re\lambda}' = \langle u'\rangle\,\lambda/\nu$) above 500.

TURBULENCE MEASUREMENTS IN LIQUIDS

The measurement of velocity fluctuations in the flow of liquids has recently become feasible with the development of the hot-film anemometer (13, 14). Interest has therefore developed both in comparing liquid turbulence with gas turbulence (15) and in studying turbulence phenomena in viscoelastic fluids (2).

The hot-film anemometer has the high strength to withstand the impact pressure of high-velocity liquids and the impact force of dirt particles (16). The primary advantage in the use of the hot-film anemometer in liquids, however, is its tendency to shed lint and dirt particles in a liquid stream. Lint collects very rapidly on a wire, wrapping itself around the wire very tightly and changing the wire calibration and frequency response drastically. Since the lint cannot wrap around a hot-film wedge probe, such collections are usually avoided by its use, allowing the use of a single calibration over long periods of time.

Very few turbulence measurements in liquids have been made, as the development of the hot-film anemometer was quite recent. All but one of the liquid turbulence investigations previous to the work described here were made in water. Several of these were made in geometries unlike a cylindrical tube (12, 13, 15, 17, 18) and will not be discussed in detail since the results are difficult to relate to the tube data.

Lee and Brodkey (19) measured the longitudinal intensity, the energy spectrum, and the microscale in the pipe flow of water using a Lintronics film probe. Their measurements were made in a 3.068-in. polyethylene pipe. Their intensity data are questionable because they experienced calibration drift during measurements, causing a slight peak at the pipe center. Calibration drift is commonly experienced in measurements in water with an uncoated probe (16).

Corino and Brodkey (20) have recently measured turbulence intensities in the turbulent flow of trichloroethylene in conjunction with visual studies of turbulence in the boundary layer. They reported good hot-film probe calibration stability in the nonconducting fluid, but their intensity results (reported at N_{Re} = 21,500 only) were low near the wall in comparison to other data (4, 5).

Martin and Johanson (21) measured turbulence intensities and made autocorrelations for water turbulence in the center of a 6-in. pipe for Reynolds numbers of 19,000 to 160,000. Their turbulence intensities are close to those obtained by Sandborn (4) in the same Reynolds number range using air in a 4-in. pipe. They used their autocorrelations to calculate integral scale values, which are compared with the results of this investigation in the discussion.

Lindgren (22) measured turbulence intensities in a 127-mm. pipe using a 2-mm. long film wedge probe in water. His data, though extensive, are quite scattered.

APPARATUS AND EXPERIMENTAL PROCEDURE

The measurements of longitudinal turbulence intensities, energy spectra, and autocorrelations in the flow of organic solvents were done in the pipe flow unit described in detail by Hershey (1) and Hershey and Zakin (23). Measurements were made in smooth wall steel tubes of 2- and 1-in. I.D. with lengths of 150 and 275 diameters, respectively. As shown in Figure 1, the unit had a 100-gal. surge tank which fed either

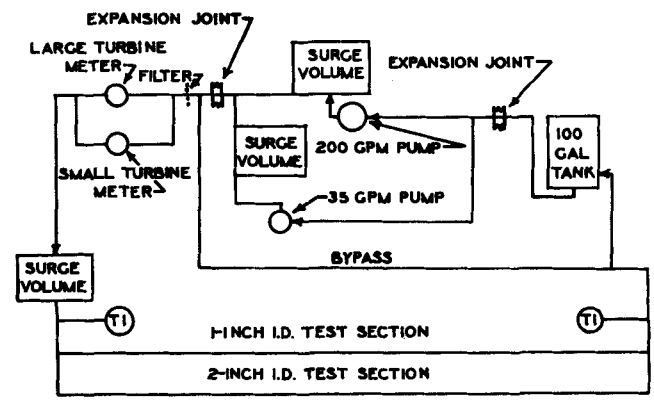

Fig. 1. Schematic diagram of pipe flow apparatus.

a 35- or a 200-gal./min. Viking gear pump. Each pump had a surge damping cylinder holding 0.1 cu. ft. of air. In addition a 0.3-cu. ft. surge damping cylinder was located at the inlet manifold to the measurement tubes.

The control of fluid temperature is critical in hot-film anemometry in liquids because of the low overheat ratios† used. Temperature control was maintained within ± 0.05°C. by heated water flowing in a coil in the surge tank. The temperature sensor used was a Jumo water bath thermoregulator with a precision of ± 0.01°C. The temperature was read at the measurement tube inlet and outlet manifolds by calibrated thermometers graduated in 0.1°C. intervals. The cyclohexane and benzene were used at 25.0°C. and the toluene at 30.0°C.

Flow rate measurements were made using either a 1½- or ¾-in. Brooks turbine meter. The flow rate through each was a linear function of the frequency of the fluctuating voltage produced by its rotating turbine. The frequency was measured with a Heath frequency meter. The turbine meters were calibrated by diverting liquid into a weigh tank.

The calibration of the hot-film anemometer was accomplished by measuring velocity profiles in turbulent flow using an impact tube. The profiles for the 2-in. tube were reported by Hershey. The velocity profiles for the 1-in. tube were reported by Patterson (*2*). All these profiles are adequately represented by the defect law $(\bar{u}_c - \bar{u})/u^* = 3.35 \ln (y/a)$. Flow rates calculated from integrated velocity profiles were within 3.0% of the measured flow rates. The impact tube velocity profiles and hot-film anemometry measurements were made using the same micrometer positioner. Hershey made friction factor measurements in the same tubes at all conditions reported here and found very close agreement with the Nikuradse (*24*) data. The average deviation was less than 2.0%.

The constant-temperature anemometer was a Disa model 55A01 with a Disa hot-film probe. The frequency response of the overall anemometer system was such that 3 decibel attenuation occurred at about 8,000 cycles/sec. for all flow conditions used. This was measured with a square wave generator built into the anemometer circuit used (*25*). The anemometer was equipped with high- and low-pass filters to eliminate unwanted signals. In practice only the low-pass filter was used to eliminate electronic noise above 20,000 cycles/sec.

The hot-film probe was a 30 deg. glass wedge 1 mm. long plated with platinum. The probe shape was similar to that described by Ling (*13*). The probe was supported by a 7-mm. rod extending through the measurement tube. The probe tip extended 3½ in. upstream from the support rod. Electrical connections were made at one end of the rod and a micrometer positioner precise to 0.001 in. was clamped to the other end. This design, with a Teflon packing used at each end of the support rod, gave the probe great rigidity.

Since organic, nonconducting solvents were used as fluids, the calibrations of the hot-film anemometer were very stable. The only cause of calibration change was the occasional collection of lint by the wedge probe. Since this occurred relatively infrequently, adequate calibrations were obtained between disturbances.

An Ampex 601-2 audio tape recorder was used to make two-channel recordings of the anemometer output. These recordings were used for the autocorrelations (with a Disa 55A06 correlator) and for the spectrum measurements [with a 34-band active band pass filter designed and built by Watson (*26*)]. The autocorrelations were made by delaying the playback of one channel of the recordings using a moveable playback head installed on the Ampex recorder. The playback delay times were accurate to ± 0.0001 sec. The zero delay time position was established by finding the position of peak correlation number (usually 0.98 to 0.99).

The band pass filter was calibrated by measuring the frequency response curves of all the bands and by determining the relative root-mean-square energy level passed by each band. Corrections for frequency response of the Ampex tape recorder were made using measured output-input ratios at frequencies from 10 to 10,000 cycles/sec.

† Overheat ratios used in this investigation were 1.1 to 1.15.

Materials

The organic solvents used were commercial grades of toluene (density, 0.856 g./cc.; viscosity, 0.518 centipoise; G. S. Robbins Co., St. Louis, Missouri), benzene (density, 0.874 g./cc.; viscosity, 0.610 centipoise; Independent Petroleum Corp., St. Louis, Missouri), and cyclohexane (density, 0.775 g./cc.; viscosity, 0.889 centipoise; G. S. Robbins Co., St. Louis, Missouri). The toluene and cyclohexane were greater than 99% pure and the benzene had a maximum boiling range of 1°C. to include 80.1°C., the boiling point of pure benzene. The toluene was used for turbulence intensity, autocorrelation, and energy spectrum measurements in both the 1- and 2-in. tubes. The benzene was used for all the above measurements in the 2-in. tube, and the cyclohexane was used for turbulence intensity measurements in the 1-in. tube.

DISCUSSION OF DATA

Longitudinal Turbulence Intensity Profiles

The hot-film anemometer was used to measure longitudinal turbulence intensities in both 1-in. and 2-in. smooth-wall tubes. In all cases traverses were made from the tube center to a position near the wall (r/a of 0.75 in the 1-in. tube and r/a of 0.85 in the 2-in. tube), moving the probe by means of the micrometer positioner. Two typical turbulence intensity tranverses are shown in Figure 2 for toluene flowing in a 2-in. tube. The intensity increased as the wall was approached as in the measurements of Sandborn and Laufer. However, since the nearest approach to the wall in this study was $r/a = 0.85$, a maximum intensity was not observed.

As shown in Figures 3, 4, and 5 for r/a of 0, 0.75, and 0.85, respectively, turbulence intensities generally increased with lower Reynolds number in a manner similar to the Laufer and Sandborn data for air and the Martin-Johanson data for water. A small diameter effect may be seen in Figures 3 and 4, with the 1-in. tube data giving slightly lower intensities. (Although this difference might be attributable to increased blockage in the 1-in. tube, the higher pressure gradient upstream of the probe support might be expected to cause higher intensities.)

The Laufer air data are in closest agreement with the data of this investigation, lying in the lower portion of the 2-in. tube data. (Laufer used only two flow rates, so the straight lines in Figures 3 and 5 simply connect two points.) The air data of Sandborn, which were measured in a 4-in. pipe, are lower than Laufer's data at the pipe center and are slightly higher near the wall. The Martin-Johanson intensities, measured in the center of a 6-in. pipe, are lower than those of this investigation. As shown in Figure 3 their data also show a stronger dependence on Reynolds number.

The water data of Lee and Brodkey and of Lindgren are not compared with the other available data, because

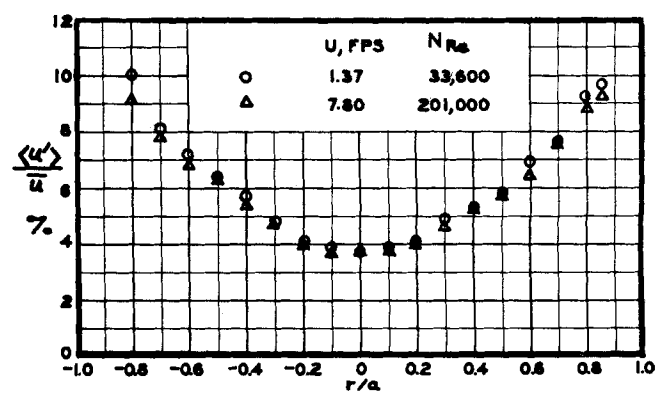

Fig. 2. Turbulence intensity profiles for toluene in a 2-in. I.D. tube.

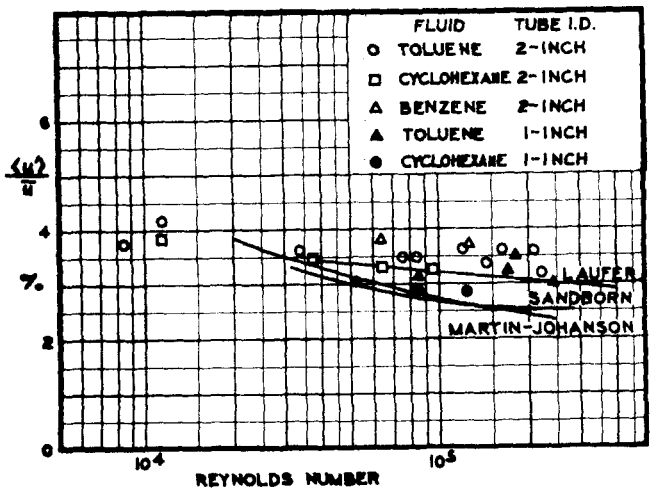

Fig. 3. Turbulence intensity at $r/a = 0.0$.

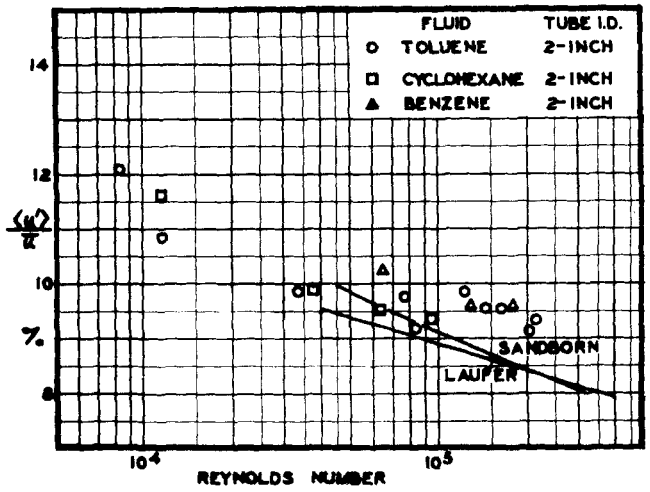

Fig. 5. Turbulence intensity at $r/a = 0.85$.

they experienced calibration drift problems with their hot-film anemometers. The turbulence intensity profile of Corino and Brodkey was radically different from all other reported profiles.

The precision of the longitudinal turbulence intensity data is indicated by its axisymmetry and the deviation from the best fit curve through the data plotted as intensity vs. N_{Re}. For most of the intensity profiles, data were obtained on both sides of the tube center to check the axisymmetry of the flowing stream. Figure 2 is typical of the symmetry for most of the profiles measured. The worst symmetry was observed for toluene at Reynolds numbers 8,240 and 11,500, where differences of about 2% in intensity values were observed for regions near opposite walls, intensity levels being about 10%. These two profiles were obtained at very low velocities where it was difficult to maintain steady flow rates with the equipment used.

The axisymmetry of the velocity profiles used in hot-film anemometer calibration was discussed in detail by Hershey. The velocity profiles showed good symmetry.

If it is assumed that there is no significant viscosity effect for the solvents used (viscosities of 0.54 to 0.89 centipoise), the mean deviation of the intensity measurements from the curve best fitting the turbulence intensity vs. Reynolds number data may be calculated. When this was done with a separate best fit curve used for the 1-in. and 2-in. diameters, the mean deviation of the intensities at the tube centers was ± 0.12%. Since the average intensity at the tube center was about 3.5%, the mean deviation was ± 3.4% of this value. The data of Martin and Johanson, with a hot-film probe for measurements in water and for one pipe size, show a mean deviation which is about ± 8% of their average value. Sandborn's data, obtained with a hot-wire probe in air, show a mean deviation from the best fit curve of about ± 1% of the average value.

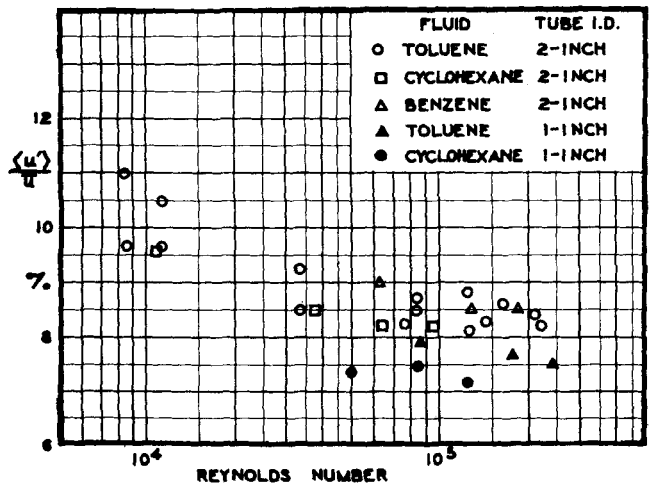

Fig. 4. Turbulence intensity at $r/a = 0.75$.

Turbulence Energy Spectra

Turbulence energy spectra typical for low viscosity liquids are shown in Figures 6 and 7. These spectra were measured in toluene in both 1-in. and 2-in. smooth-wall tubes at positions near the wall and at the tube center. Also in Figure 6 is the spectrum data of Lee and Brodkey for water at the center of a 3.068-in. pipe. (Although their turbulence intensity data were affected by drift, an energy spectrum measured from a short recording should not be seriously affected.) Considering their velocity of 1.83 ft./sec. and the trend of the toluene data with velocity, we see that the water and toluene data are in good agreement. These data illustrate the general conclusions of this investigation concerning turbulence energy spectra in round tubes:

1. There is a strong dependence of the position of the curves on bulk mean velocity. At the highest bulk mean velocity, the middle frequency range seems to show the $-5/3$ power dependence, extending the spectrum to higher frequencies. Higher Reynolds numbers are needed to *prove* the existence of the $-5/3$ log-log slope in pipe flow. The turbulence microscale Reynolds numbers $N_{Re\lambda}'$ for the toluene and benzene measurements range from 280 to 1,280, thus including the minimum $N_{Re\lambda}'$ (about 500) for the existence of an inertial subrange (region of $-5/3$ power dependence on frequency) indicated by grid turbulence measurements (*12*).

2. The energy spectra are relatively independent of tube size. At the same bulk mean velocities, the spectra obtained in 1-in. and 2-in. tubes are in close agreement (compare Figures 6 and 7).

3. The energy spectra are relatively independent of radial position from the center to $r/a = 0.85$. Since the probe used did not allow measurements closer to the wall, the dependence of spectra on position could not be measured in $0.85 > r/a > 1.0$. When Laufer's spectrum data for air in a 10-in. pipe are expressed as a function of frequency (rather than wave number) large changes occur only within 0.1 a of the wall.

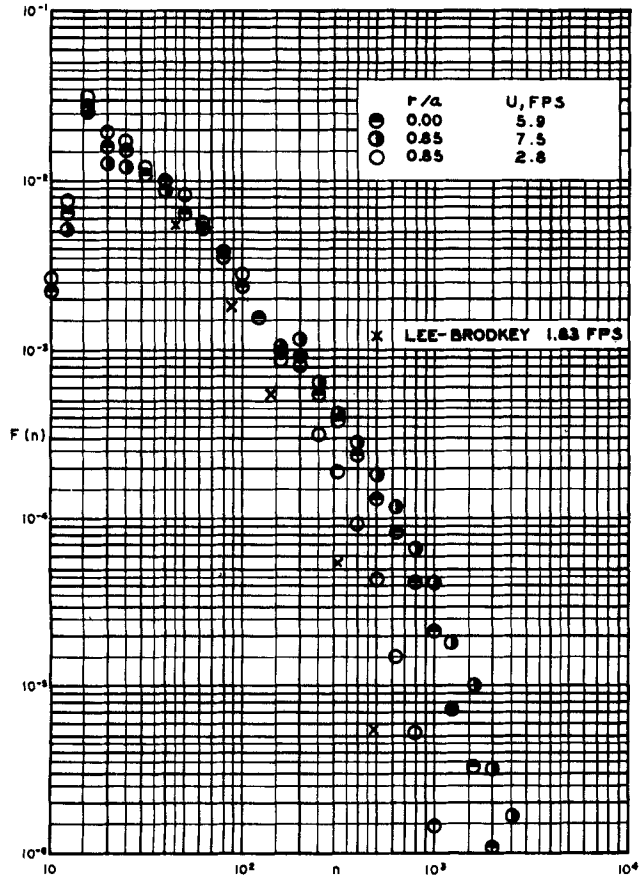

Fig. 6. Turbulent energy spectra in a 2-in. I.D. tube for toluene.

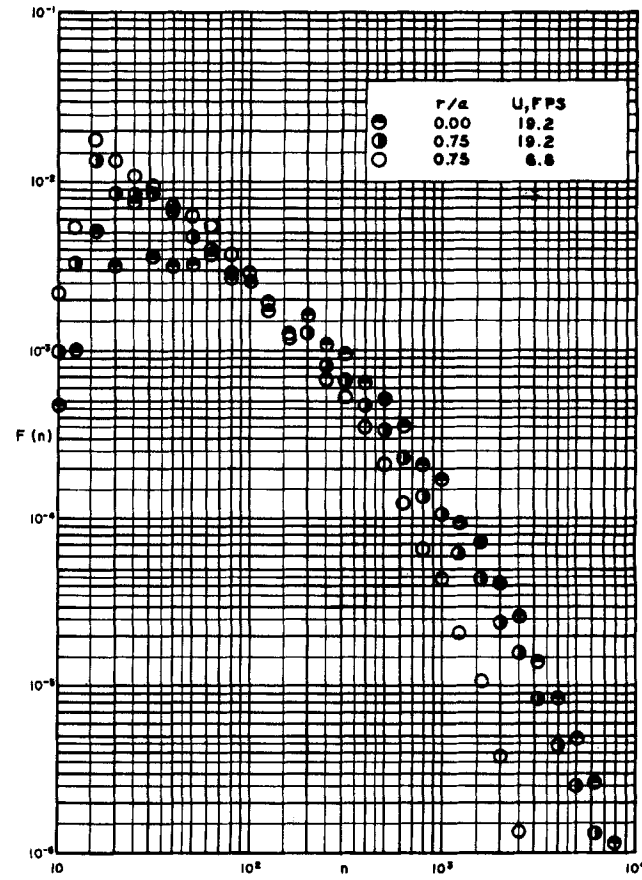

Fig. 7. Turbulent energy spectra in a 1-in. I.D. tube for toluene.

4. The spectra at lowest bulk mean velocities approach but do not reach the -7 power dependence on frequency at high frequencies predicted by Heisenberg's transfer theory. The beginning of the steep region occurs at higher frequencies as velocity is increased.

The frequency of maximum energy dissipation was obtained for each of the energy spectra by plotting the isotropic dissipation spectra $n^2 F(n)$ vs. n. The data showed fairly sharp maxima and the corresponding frequencies n_{max} could be estimated accurately. Figure 8 is a plot of n_{max} vs. the bulk mean velocity U. For these low viscosity liquids n_{max} is approximately proportional to bulk mean velocity to the 1.4 power. Such information will be shown in a later paper to be useful in predicting the extent of drag reduction in polymer solutions.

Comparisons of the turbulent energy spectra measured with the use of the audio recordings with directly measured spectra (without recording) and spectra measured with the use of pulse duration modulation recordings (made with a Lyrec TR-60 autocorrelation tape recorder loaned by Zitzewitz Engineering Associates, Inc., Wyckoff, New Jersey) showed that they were attenuated in the low-frequency range (below 15 cycles/sec.) only. The repeatibility of the spectrum data was good, as evidenced by comparison of solvent spectra measured at different times.

Length corrections were not made on the spectra. Gibson and Schwarz indicated that they did not make such corrections, because the existing wire length correction methods did not necessarily apply to a film probe. (Their probe was similar to the Disa probe used here.) Although the Kolmogoroff hypotheses are based on local isotropy at high frequencies, the possibility of anisotropy even at the highest frequencies exists for these spectra, since they were measured in pipe flow. This further complicates the use of a length correction.

Approximate length corrections based on the Betchov (27) method show that corrections apply to these spectra only at the highest frequencies and these raise the spectra only a small amount. Such corrections have negligible effect on microscale calculated with Equation (10).

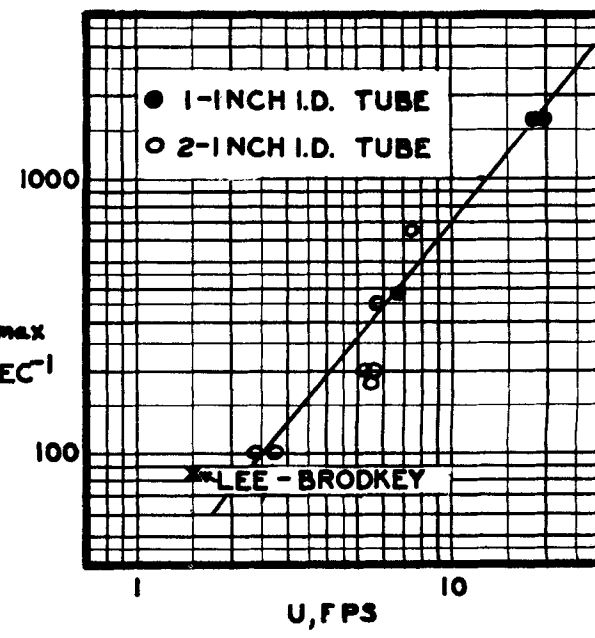

Fig. 8. Frequency of maximum energy dissipation.

TABLE 1. INTEGRAL SCALE AND MICROSCALE

Tube size in., I.D.	Fluid	r/a	Bulk mean velocity, ft./sec.	Measured integral scale, ft.	Calculated integral scale, Eq. (11)	Microscale, ft.
2.0	Benzene	0.0	5.5	0.0143	0.0161	0.0102
		0.85	5.5	0.0152		0.0077
		0.85	2.5	0.0079		0.0061
2.0	Toluene	0.0	5.9	0.0161	0.0178	0.0078
		0.85	7.5	0.0157		0.0057
		0.85	2.8	0.0074		0.0055
		0.85	2.8	0.0090 (p.d.m.)		0.0063 (p.d.m.)
1.0	Toluene	0.05	19.2	0.0131	0.0110	0.0052
		0.75	19.2	0.0275		0.0058
		0.75	6.8	0.0130		0.0052

Integral Scale

Integral scale values were calculated from the energy spectra measured for the turbulent flow of organic solvents by first transforming the spectra to autocorrelations (2) and then by using Equation (6). This method was more accurate than using autocorrelations measured by the Ampex audio tape recorder because of the difficulty in correcting the autocorrelation data for poor low-frequency response. The integral scale calculations used 0.8 $\bar{u}_c$ as the convection velocity for all measurements.

The accuracy of the integral scale measurements with the audio tape recorder used was demonstrated by comparison with direct measurements (without recording) and with measurements from p.d.m. (pulse duration modulation) recordings. The audio integral scale values were found to be 10 to 20% low because of the loss of signal below 15 cycles/sec.

The integral scale values for the flow of toluene and benzene are shown in Table 1. The values for the 1- and 2-in. tubes ranged between 0.0079 and 0.0275 ft. for bulk mean velocities of 2.5 to 19.2 ft./sec. For a given radial position in a given tube, integral scale increased with bulk mean velocity to a power less than one. There was little radial location effect in the 2-in. tube. The low value (0.0131 ft.) near the center of the 1-in. pipe is considered erroneous, because the spectrum (Figure 7) appears to have been inadequately corrected for frequency response.

Martin and Johanson integrated their autocorrelation curves to obtain integral scales for the flow of water in the center of a 6-in. pipe. Their data were fit by the equation

$$L_x = 1.692 \times 10^{-2}\, a (N_{Re} \times 10^{-3})^{0.509} \qquad (11)$$

where L_x is in feet. The comparison in Table 1 of measured integral scale values and values calculated with Equation (11) shows that the $(U^{0.5}\, a^{1.5})$ product in the Martin-Johanson relationship probably does not properly correlate data with varying pipe diameter and velocity. The diameter effect appears to be too large and the velocity effect may be too small.

Microscale

Microscale, which is an indication of the proportion of high-frequency energy in the spectrum, was calculated by integrating the dissipation spectrum according to Equation (10). These values are offered to show their magnitude in liquids, which have not been previously reported. Microscale showed no clear trend with velocity. This confirms Laufer's (28) measurements in a 4-in. channel, which showed only slight increases of microscale with decreasing velocity. Data for a greater range of tube sizes are needed to determine the dependence of the centerline microscale on tube size.

Near the wall microscale values for both tube sizes and all velocities approach the same value. Since microscale is approximately inversely proportional to the frequency of maximum energy dissipation [see Equation (10)], the weak dependence of microscale on bulk mean velocity indicates that the frequency of maximum energy dissipation should be roughly proportional to bulk mean velocity. As shown above it is actually proportional to bulk mean velocity to the 1.4 power for these data.

ACKNOWLEDGMENT

This work was partially supported by a research grant from the National Aeronautics and Space Administration (NGR 26-003-003) which is gratefully acknowledged. A National Science Foundation Equipment Grant toward the purchase of the p.d.m. tape recorder is also acknowledged. We also appreciate the assistance of the Socony Mobil Oil Company which provided an equipment grant for this research. Gary K. Patterson was supported during this work by a National Science Graduate Fellowship. The experimental help of Dr. H. C. Hershey and J. M. Rodriguez was invaluable.

NOTATION

a = tube radius
$E_x(n)$ = one-dimensional energy spectrum function
$f(\delta)$ = axial space correlation function
$F_x(n)$ = normalized one-dimensional energy spectrum function
L_x = integral scale in axial direction
n = frequency
p_o = reference pressure
$\bar{p}$ = time average pressure
r = radial distance from center
N_{Re} = Reynolds number, UD/ν
$N_{Re\lambda}'$ = turbulence microscale Reynolds number, $<u'>\lambda/\nu$
$R(\tau)$ = autocorrelation function
t = time
$\bar{u}$ = local time average velocity
$\bar{u}_c$ = time average velocity at pipe center
$\bar{u}_\infty$ = free-stream velocity in a wind tunnel
u', v', w' = fluctuating components of velocity in axial, radial, and tangential directions
$\overline{u'v'}$ = Reynolds stress
$<u'>$ = root-mean-square of fluctuating component of velocity, equivalent to $\sqrt{\overline{(u')^2}}$
u^* = friction velocity, $\sqrt{\tau_w/\rho}$
U = bulk mean velocity in a pipe
W = rate of turbulent energy dissipation

x = axial coordinate
y = distance from pipe wall

Greek Letters

δ = distance between correlation points
λ_f = longitudinal microscale (in axial direction)
ρ = density
ν = kinematic viscosity
τ = delay time
τ_w = shear stress at the wall

LITERATURE CITED

1. Hershey, H. C., Ph.D. thesis, Univ. Missouri at Rolla (1965).
2. Patterson, G. K., Ph.D. thesis, Univ. Missouri at Rolla (1966).
3. Hinze, J. O., "Turbulence," McGraw-Hill, New York (1959).
4. Sandborn, V. A., *Natl. Advisory Comm. Aeronaut. Tech. Note 3266* (1955).
5. Laufer, John, *Natl. Advisory Comm. Aeronaut. Tech. Rept. 1174* (1953).
6. Taylor, G. I., *Proc. Royal Soc. (London)*, **A151**, 421 (1935).
7. *Ibid.*, **A164**, 476 (1938).
8. Favre, A., J. Gaviglio, and R. Dumas, *Recherche Aeronaut.* No. 32 (Mar.-Apr., 1953); translation in *Natl. Advisory Comm. Aeronaut. Tech Memo 1370* (1955).
9. Sternberg, J., *J. Fluid Mech.*, **13**, 243 (1962).
10. Kolmogoroff, A. N., *Compt. Rend. (Dokl.) Acad. Sci. URSS*, **30**, 301 (1941); translated in S. K. Friedlander, and L. Topper, "Turbulence," Interscience, London (1961).
11. Heisenberg, W., *Z. Phys.*, **124**, 628 (1948).
12. Gibson, C. H., and W. H. Schwarz, *J. Fluid Mech.*, **16**, 365 (1963).
13. Ling, S. C., Ph.D. thesis, State Univ. Iowa, Iowa City (1955).
14. ———, *J. Basic Eng.*, 629 (Sept., 1960).
15. Rosler, R. S., and S. G. Bankoff, *A.I.Ch.E. J.*, **9**, 672 (1963).
16. Rundstadler, P. W., Jr., paper presented at A.S.M.E. Symp. Unsteady Flow, Hydraulic Div. Conf., Worcester, Mass. (May, 1962).
17. Gibson, M. M., *J. Fluid Mech.*, **15**, 161 (1963).
18. Grant, H. L., R. W. Stewart, and A. Moilliet, *ibid.*, **12**, 241 (1962).
19. Lee, Jon, and R. S. Brodkey, *A.I.Ch.E. J.*, **10**, 187 (1964).
20. Corino, E. R., Ph.D. thesis, Ohio State Univ., Columbus (1965).
21. Martin, G. Q., and L. N. Johanson, *A.I.Ch.E. J.*, **11**, 30 (1965).
22. Lindgren, E. R., *Tech. Rept. No. 1*, Bureau Ships Gen. Hydro. Res. Progr. S-R009 01 01, Res. Contr. Nonr 2595(05) (1965).
23. Hershey, H. C., and J. L. Zakin, *Ind. Eng. Chem. Fundamentals*, accepted for publication.
24. Nikuradse, J., *VDI-Forschungsheft*, 356 (1932).
25. "Operation Manual for Disa Constant Temperature Anemometer," Disa Electronik, Herlev, Denmark (Aug., 1963).
26. Watson, T. B., M.S. thesis, Univ. Missouri at Rolla (1965).
27. Betchov, R., *J. Fluid Mech.*, **3**, 205 (1957).
28. Laufer, John, *Natl. Advisory Comm. Aeronaut. Tech. Rept. 1053* (1949).

Manuscript received June 13; revision received September 30, 1966; paper accepted October 1, 1966. Paper presented at A.I.Ch.E. Detroit meeting.

Dynamics of a Tubular Reactor with Recycle: Part II. Nature of the Transient State

M. J. REILLY and R. A. SCHMITZ
University of Illinois, Urbana, Illinois

A theoretical study of the transient state of a plug-flow tubular reactor with recycle is presented for a model in which axial dispersion of heat and mass is negligible. A qualitative description of the temporal behavior near the steady state is obtained from an analysis of the linearized transient equations, and some large-scale transient characteristics are studied by means of numerical solution of the nonlinear transient equations. A cursory study of the application of the Liapunov's direct method to predict regions of asymptotic stability is also presented. Numerical examples illustrate sustained oscillatory behavior as well as the transient nature of systems with multiple steady states.

In a previous paper (*1*) the stability of the steady state of a plug-flow tubular reactor with recycle was analyzed. It was shown that stability or instability to small disturbances could be rigorously determined immediately upon attainment of a steady state solution by a Newton-Raphson iterative procedure. Numerical examples were presented which illustrated the possible existence of unstable steady states.

The purpose of this paper is to investigate the complete transient nature of the reactor-recycle system. The methods utilize the notion of a phase plane representation of the transient outlet state. The study of the behavior in the phase plane is based first on linearized transient equations and second on numerical solution of the nonlinear transient equations for some numerical examples. Finally, results obtained by applying the Liapunov's direct method to predict regions of asymptotic stability are presented and compared with those obtained by numerical solution of the transient equations.

M. J. Reilly is at Carnegie Institute of Technology, Pittsburgh, Pennsylvania.